

**Contract No:**

This document was prepared in conjunction with work accomplished under Contract No. DE-AC09-08SR22470 with the U.S. Department of Energy (DOE) Office of Environmental Management (EM).

**Disclaimer:**

This work was prepared under an agreement with and funded by the U.S. Government. Neither the U. S. Government or its employees, nor any of its contractors, subcontractors or their employees, makes any express or implied:

- 1 ) warranty or assumes any legal liability for the accuracy, completeness, or for the use or results of such use of any information, product, or process disclosed; or
- 2 ) representation that such use or results of such use would not infringe privately owned rights; or
- 3) endorsement or recommendation of any specifically identified commercial product, process, or service.

Any views and opinions of authors expressed in this work do not necessarily state or reflect those of the United States Government, or its contractors, or subcontractors.

**PVP2020-21774**

## CISCC EXPERIMENT OF A LARGE PLATE SECTIONED FROM A SPENT NUCLEAR FUEL CANISTER

**Andrew J. Duncan, Poh-Sang Lam<sup>1</sup>, Robert L. Sindelar**  
 Savannah River National Laboratory  
 Aiken, South Carolina, USA

### ABSTRACT

*As a long-term demonstration of chloride-induced stress corrosion cracking (CISCC) driven by welding residual stress (WRS), a large section (approximately 51×46 cm with thickness 16 mm and weight about 30 kg), which contains a circumferential weld, was cut from a full-size mockup canister. Through-wall and part-through-wall (surface) starter cracks, either parallel or perpendicular to the weld, were fabricated with electrical discharge machining (EDM) in the weld region. The stress intensity factors ( $K_I$ ) for each machined starter crack under canister WRS were estimated so as to provide insight into the propensity for crack initiation and growth. Dry salt was applied over these machined cracks on the surface of the large plate and natural deliquescence was allowed to take place at room temperature and 75% RH. This test has been on-going for ten months and the evolution of general corrosion near the starter cracks is monitored and documented; no CISCC has been observed. Two EDM starter cracks have been isolated for five months for a simultaneous experiment with extra salt loading; additional deliquescence and significant corrosion activity have been observed.*

Keywords: Spent nuclear fuel (SNF), Chloride-induced stress corrosion cracking (CISCC), Deliquescence, Stainless steel canister, Welding residual stress (WRS), Starter crack, Salt loading, Stress intensity factor

### 1. INTRODUCTION

Stress corrosion cracking (SCC) is the major concern in the dry storage of spent nuclear fuel (SNF) for the potential of developing through-wall penetration that breaches the confinement boundary provided by the storage canisters, especially for those in the Independent Spent Fuel Storage Installations (ISFSIs) in the coastal regions with chloride-rich

environments. A stainless steel plate of 51×46 cm containing a circumferential weld was cut from a full-size mockup SNF canister [1] for conducting a chloride-induced stress corrosion cracking (CISCC) experiment using the “large plate” as the test specimen. A set of part-through-wall and through-wall starter cracks were fabricated by electrical discharge machining (EDM) in the welding residual stress (WRS) region. Stress intensity factors were calculated with American Petroleum Institute (API) 579 procedures [2,3] to provide insight into crack initiation and growth under WRS field. Dry artificial sea salt of 2.3 g/m<sup>2</sup> chloride was applied on the large plate surface and allowed to deliquesce naturally under laboratory controlled 75% relative humidity (RH) at an ambient room temperature of 22 °C [3]. General corrosion including pitting has occurred, but cracking has not been observed after ten months of exposure. Two EDM starter cracks were isolated and loaded with an order of magnitude increase in salt loading. Additional deliquescence and significant corrosion activity have been observed but, to date, there are still no visual indications of cracking. This paper describes the test conditions of the experiment and an explanation of the results.

## 2. LARGE PLATE DEMONSTRATION OF CISCC

### 2.1. Materials and Experimental Setup

The behavior of steel susceptible to SCC can be described in terms of its crack growth rate (CGR) and threshold stress intensity factor ( $K_{ISCC}$ ) for environmental cracking. These properties can be determined by the bolt-load compact tension (CT) tests as summarized by Lam, Sindelar, and Duncan [3-6] using ASTM E1681, “Standard Test Method for Determining Threshold Stress Intensity Factor for Environment-Assisted Cracking of Metallic Materials.” For non-stress relieved vessels subject to WRS loading in corrosive environments, such as the

<sup>1</sup> Contact author: ps.lam@srnl.doe.gov

high-level nuclear waste tanks, large plate tests have been carried out to demonstrate the cracking behavior on the structural level [7-9]. In the present case, the phenomenon of CISC during long-term storage of the SNF canisters is investigated by using a

large stainless steel plate (dual certified 304/304L, Table 1) obtained from the same full-size mockup canister where the bolt-load CT specimens were harvested from [3-6].

**TABLE 1: MATERIAL CHEMICAL COMPOSITIONS FOR SANDIA MOCKUP CANISTER (wt.%) [1]**

Materials	C	Co	Cr	Cu	Mn	Mo	N	Ni	P	S	Si
Base Metal 304/304L	0.0223	0.1865	18.1	0.4225	1.7125	0.318	0.0787	8.027	0.0305	0.0023	0.255
Weld Filler 308L (Lot 1)	0.014	–	19.66	0.16	1.7	0.11	0.058	9.56	0.025	0.010	0.39
Weld Filler 308L (Lot 2)	0.012	–	19.71	0.192	1.730	0.071	0.053	9.75	0.024	0.012	0.368

This plate was sectioned through a region of the canister that contains a circumferential weld and has a planar dimension of 51×46 cm with a thickness of 16 mm and its weight is about 30 kg (see Figure 1). The size of the sectioned plate was carefully determined from a series of finite element calculations to minimize the redistribution or relieving of WRS due to cutting<sup>†</sup>. In a separate study by Wang et al. [10], neutron diffraction was used to determine the remaining WRS in a similar but smaller plate, which was also cut from the same mockup canister but contains an axial weld. Their experimental data confirmed that most of the as-welded residual stresses were retained in the sectioned plate. Therefore, it is reasonable to assume that the residual stresses in the large plate would be similar to those reported by Enos and Bryan (experiment) [1] and by Gim et al. (finite element simulation) [11].

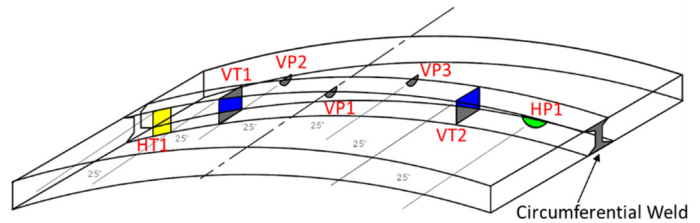


**FIGURE 2: EDM STARTER CRACKS SCHEMATICS ALONG THE CIRCUMFERENTIAL WELD**

## 2.2. Starter Cracks

Starter cracks (aka seed cracks or machined cracks), have been introduced to the large plate in the weld region by EDM and are currently being exposed to a CISC environment in 75% RH at room temperature since May 2019. The assumption of this demonstration is that the plate has existing stress corrosion cracks that have already initiated, and the unknown incubation time for crack initiation is ignored. Therefore, the objective of the demonstration is to verify the potential for continual crack growth as well as the crack growth characteristics (such as direction and branching, etc.); and if possible, to quantify the average CGR. Sensors, such as traditional ultrasonic test (UT), phased array ultrasonic test (PAUT), or other non-destructive examination (NDE) techniques, may be used to detect and characterize crack growth.

There are seven starter cracks machined into the large plate with a circumferential weld, as schematically shown in Figure 2. Note that the starter crack tips are located in the weld and the heat affected zone (HAZ) region. The designations and descriptions of these EDM starter cracks are:

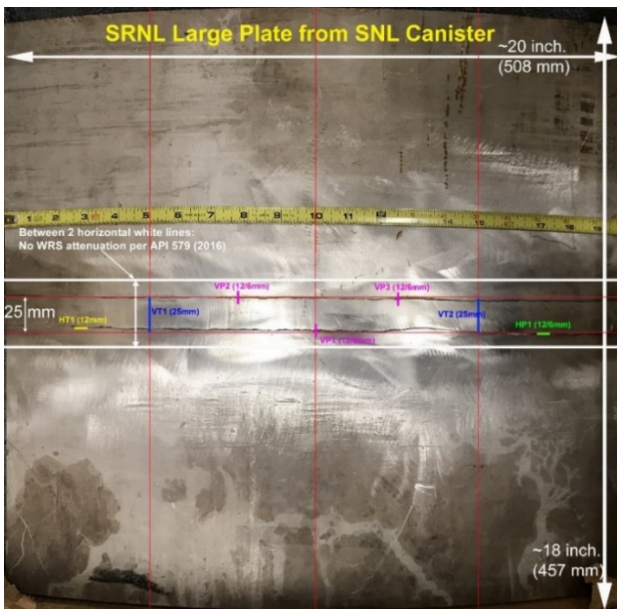


**FIGURE 1: LARGE PLATE CUT FROM A CANISTER WITH AN AS-FABRICATED CIRCUMFERENTIAL WELD AND THE LOCATIONS OF EDM STARTER CRACKS FOR CISC TEST**

<sup>†</sup> Bryan, C. (Sandia National Laboratories) to Sindelar, R. L., (Savannah River National Laboratory) email communication, August 14, 2018.

- (a) VT1, VT2: through-wall crack across the weld, crack length = 25 mm;
- (b) HT1: through-wall crack parallel to the weld edge, crack length = 12 mm;
- (c) VP1, VP2, VP3: semi-circular part-through-wall crack (surface crack) perpendicular to the weld edge, crack length = 12 mm and crack depth = 6 mm;
- (d) HP1: semi-circular part-through-wall crack (surface crack) parallel to the weld edge, crack length= 12 mm and crack depth = 6 mm.

The through-wall cracks (VT1, VT2, and HT1) were fabricated with EDM wires of 0.25 mm (0.010 in.) diameter (65% copper and 35% zinc). The resulting kerf on the plate surface (corresponding to the outer surface of the SNF canister) is less than 0.43 mm by measurement and by estimation based on wire/electrode diameters and literature data. For the semi-circular, part-through-wall cracks (VP1, VP2, VP3, and HP1), graphite ram EDM electrodes with width 0.51 mm (0.02 in.) were used. The kerf on the plate surface is less than 0.81 mm.

### 2.3. Experimental Apparatus

Artificial sea salt was prepared by following the procedure recommended in ASTM D1141, “Standard Practice for the Preparation of Substitute Ocean Water,” then deposited on the outer surface of the plate with an air brush. The salt coating procedure, as outlined in ASTM G41, “Standard Practice for Determining Cracking Susceptibility of Metals Exposed under Stress to a Hot Salt Environment,” was used to create an evenly distributed salt layer over the plate surface. The estimated salt load on the surface was 2.3 g/m<sup>2</sup> chloride (dry). Based on the research conducted at Central Research Institute of Electric Power Industry (CRIEPI) in Japan, for example, by Shira et al. [12], the threshold salt load was reported as 0.3 g/m<sup>2</sup> for SCC in stainless steel S30403. Using the CRIEPI model for salt deposition on a canister with initial emplacement temperature at 89 °C near the bottom plate and with the airborne chloride concentration of 20 µg/m<sup>3</sup>, it would require a century to reach that threshold value [12]. The salt load of 2.3 g/m<sup>2</sup> used in this test is well above the threshold value. It was intended to potentially accelerate the SCC to occur. Note that the salt load is within the reasonable levels recommended in ASTM G41 (0.155 to 155 g/m<sup>2</sup>) by repetitive spray-drying cycles. Figure 3 shows the large plate after salt spray and drying.

A transparent polycarbonate (LEXAN™) box (enclosure) with an outside dimension of 56×53×15 cm with wall thickness 12.7 mm (0.5 in.) was constructed to house the large stainless steel plate which is supported by a riser over a salt bed with saturated NaCl. Based on ASTM E104, “Standard Practice for Maintaining Constant Relative Humidity by Means of Aqueous Solutions,” a constant 75% RH environment would be

maintained inside the water-tight enclosure at room temperature (Figure 4).

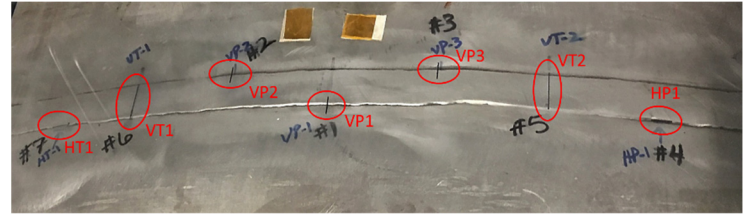
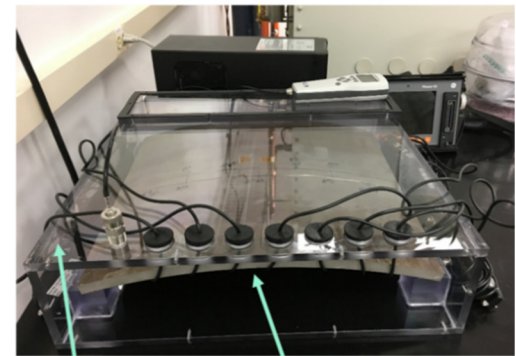


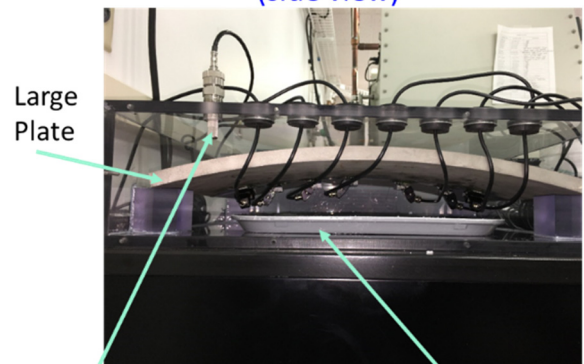
**FIGURE 3:** LARGE PLATE WITH EDM STARTER CRACKS AFTER SALT SPRAY AND DRYING

Large Plate Test Setup  
(top view)



Large Plate  
Transparent Lexan Box  
(a)

Large Plate Test Setup  
(side view)



Large Plate  
Salt Tray: ASTM E104 Saturated NaCl for RH Control  
Temperature & RH Probe  
(b)

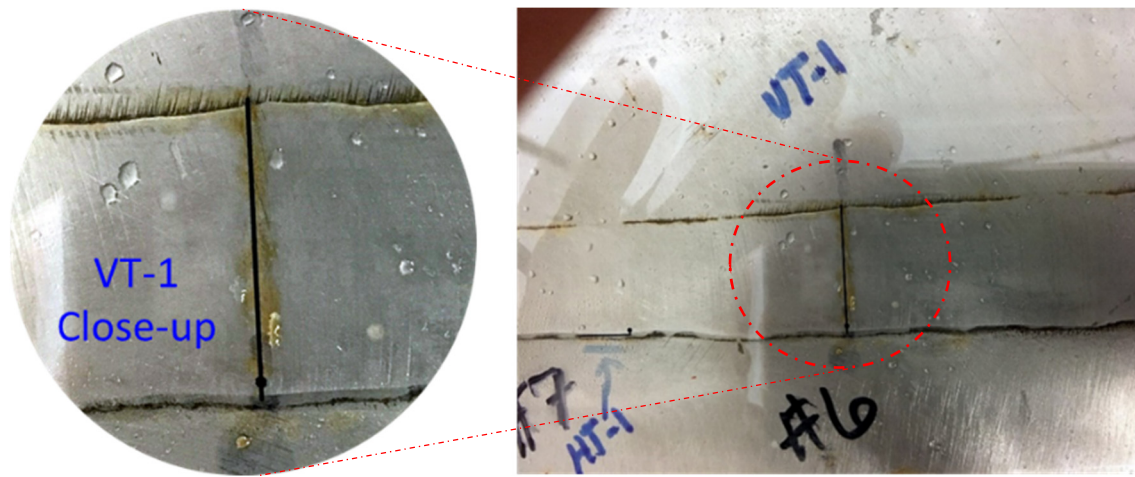
**FIGURE 4:** EXPERIMENTAL SETUP OF THE LARGE PLATE CISCC TEST UNDER NATURALLY DELIQUESCING SEA SALT AT ROOM TEMPERATURE AND 75% RH: TOP VIEW (a) AND FRONT VIEW (b)

### 3. EXPERIMENTAL OBSERVATIONS

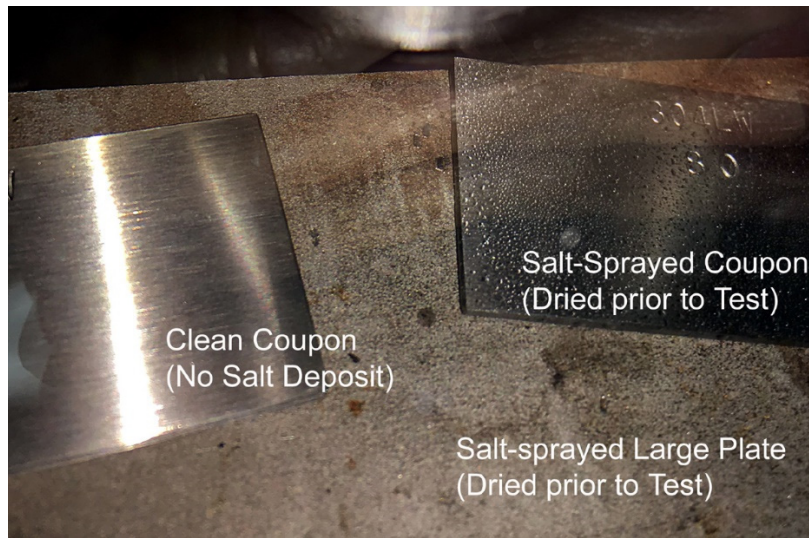
The test was initiated on May 8, 2019. The temperature and RH reached equilibrium quickly. In a few hours, numerous liquid droplets were observed on the top surface of the test plate. The closeup image near the starter crack VT1 is shown in Figure 5a. To verify that this was indeed natural deliquescence rather than water vapor condensation, two separate small stainless steel coupons were inserted into the polycarbonate enclosure on top of the large plate but remote from the weld (Figure 5b): one coupon was treated with salt spray and drying using exactly the same procedure as preparing the large plate for test; and the other coupon was clean and free from dry salt deposit. Like the large plate, the small coupon with dry salt developed liquid droplets on the surface, but the other (clean) coupon remained dry (Figure

5b). Therefore, it can be concluded that deliquescence was indeed taking place on the large plate surface. On the other hand, a continuous “liquid film” condition as originally expected was not observed. It is possible that micro-droplets could have been formed on the plate surface surrounding the more visible liquid droplets. This speculation cannot be verified with unaided eyes.

The large plate test has been periodically examined and the starter cracks have been documented with digital images in search of evidence of SCC. The evolution of the starter cracks and their immediate vicinities, observed from May 9 to October 16, 2019, is shown in Figure 6. It can be seen that the general corrosion is progressively developed, especially along the weld and the base metal interface. No CISCC cracking extending from the starter cracks has been observed to date.



(a)



(b)

**FIGURE 5:** DELIQUESCENT OCCURRED IN HOURS AND FORMING NUMEROUS LIQUID DROPLETS (a) AND ADDITIONAL COUPONS USED TO DEMONSTRATE THE PHENOMENON (b)

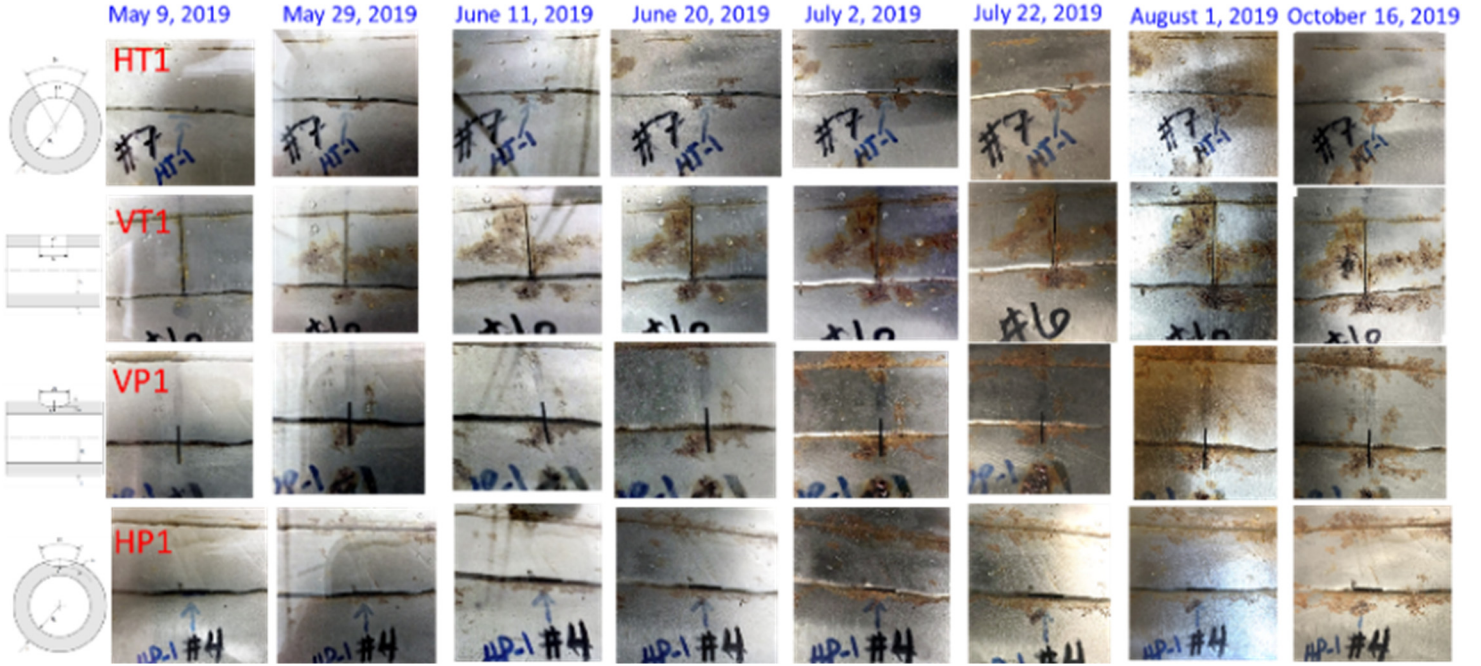


**FIGURE 6:** EVOLUTION OF CHLORIDE-INDUCED CORROSION NEAR THESE CRACKS DURING 5-MONTH EXPOSURE AT ROOM TEMPERATURE AND 75% RH

#### 4. CALCULATION OF STRESS INTENSITY FACTORS FOR STARTER CRACKS IN LARGE PLATE

Mode I stress intensity factor ( $K_I$ ) is usually calculated to provide insight for the tendency of crack propagation. For the current large plate testing,  $K_I$  has been evaluated for each starter crack under WRS loading (Figures 7-10). Korea University (KU), under the I-NERI [13] joint project, used API 579 Fitness-for-Service procedures (2007) [2] to obtain the stress intensity factor solutions [3]. The general procedure of the calculation can be described as:

- 1) Perform a 4<sup>th</sup>-order polynomial curve fitting for the WRS ( $\sigma$ ) measured by Sandia National Laboratories [1]:

$$\sigma(x) = \sigma_0 + \sigma_1 \left(\frac{x}{t}\right) + \sigma_2 \left(\frac{x}{t}\right)^2 + \sigma_3 \left(\frac{x}{t}\right)^3 + \sigma_4 \left(\frac{x}{t}\right)^4$$

where  $\sigma_i$  ( $i=0$  to 4) are the coefficients of the 4<sup>th</sup>-order polynomial,  $t$  is the canister wall thickness, and  $x$  is the through-wall coordinates with  $x=0$  at either the outer surface or inner surface, depending on the crack type (through-wall or part-through-wall) – see Figures 7-11 and the definitions of coordinate system in API 579 [2].

- 2) Calculate the stress intensity factor ( $K_I$ ) based on the formulation provided by API 579 [2].

Note that for this large plate testing with a circumferential canister weld (Figure 1), only the WRS parallel to the weld

(denoted by RS2) and perpendicular to the weld (RS3) are relevant for opening the cracks.

The  $K_I$  evaluation equation for each EDM starter crack (assuming a sharp crack) and the corresponding WRS and its curve-fitting coefficients can be found from (i) to (iv) and Figures 7-10 below. Both WRS measured at the weld centerline (WCL) and at the HAZ were considered in the calculation:

- (i) Through-Wall Crack, Longitudinal Direction (VT1 and VT2 – see Figure 2)

$$K_I = \left[ \{ \sigma_m + p_c \} G_0 + \sigma_b (G_0 - 2G_1) \right] \sqrt{\pi c}$$

where  $\sigma_m$  is the membrane stress component,  $\sigma_b$  is the bending stress component,  $p_c$  is the crack face loading and is zero in the current case, and the influence coefficients  $G_0$  and  $G_1$  are tabulated in API 579 [2]. The WRS is shown in Figure 7.

- (ii) Surface Crack, Longitudinal Direction (VP1, VP2, and VP3 – see Figure 2)

$$K_I = \left[ G_0(\sigma_0 + p_c) + G_1\sigma_1 \left(\frac{a}{t}\right) + G_2\sigma_2 \left(\frac{a}{t}\right)^2 + G_3\sigma_3 \left(\frac{a}{t}\right)^3 + G_4\sigma_4 \left(\frac{a}{t}\right)^4 \right] \sqrt{\frac{\pi a}{Q}}$$

Similar to (i), all symbols are defined in API 579 [2]. The WRS is shown in Figure 8.

(iii) Through-Wall Crack, Circumferential Direction (HT1 – see Figure 2)

$$K_I = \left[ \{ \sigma_m + p_c \} G_0 + \sigma_b (G_0 - 2G_1) \right] \sqrt{\pi c}$$

Similar to (i), all symbols are defined in API 579 [2]. The WRS is shown in Figure 9.

(iv) Surface Crack, Circumferential Direction (HP1 - Figure 2)

$$K_I = \left[ G_0 (\sigma_0 + p_c) + G_1 \sigma_1 \left( \frac{a}{t} \right) + G_2 \sigma_2 \left( \frac{a}{t} \right)^2 + G_3 \sigma_3 \left( \frac{a}{t} \right)^3 + G_4 \sigma_4 \left( \frac{a}{t} \right)^4 \right] \sqrt{\frac{\pi a}{Q}}$$

Similar to (i), all symbols are defined in API 579 [2]. The WRS is shown in Figure 10.

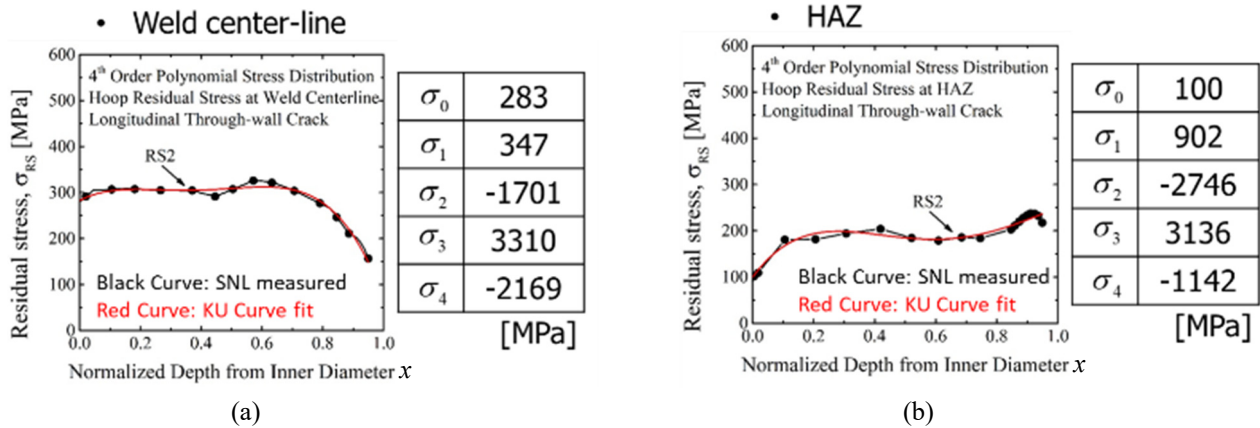


**FIGURE 7:** CURVE-FITTING OF THE WELDING RESIDUAL STRESSES AT WCL (a) AND IN HAZ (b): WRS PARALLEL TO THE CIRCUMFERENTIAL WELD: RS2;  $x=0$  AT THE CANISTER INNER SURFACE (Courtesy of Korea University under I-NERI/USA-ROK [1, 13])

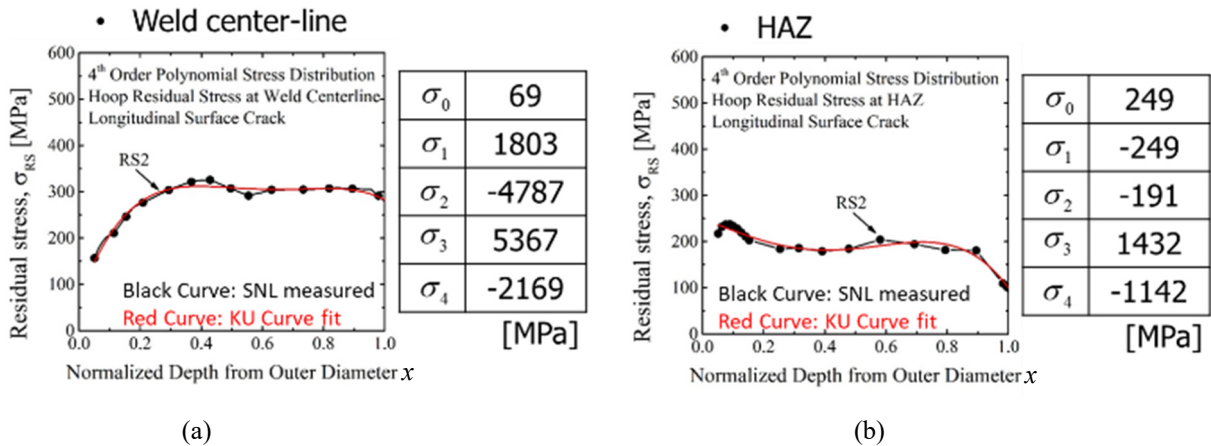


**FIGURE 8:** CURVE-FITTING OF THE WELDING RESIDUAL STRESSES AT WCL (a) AND IN HAZ (b): WRS PARALLEL TO THE CIRCUMFERENTIAL WELD: RS2;  $x=0$  AT THE CANISTER OUTER SURFACE (Courtesy of Korea University under I-NERI/USA-ROK [1, 13])

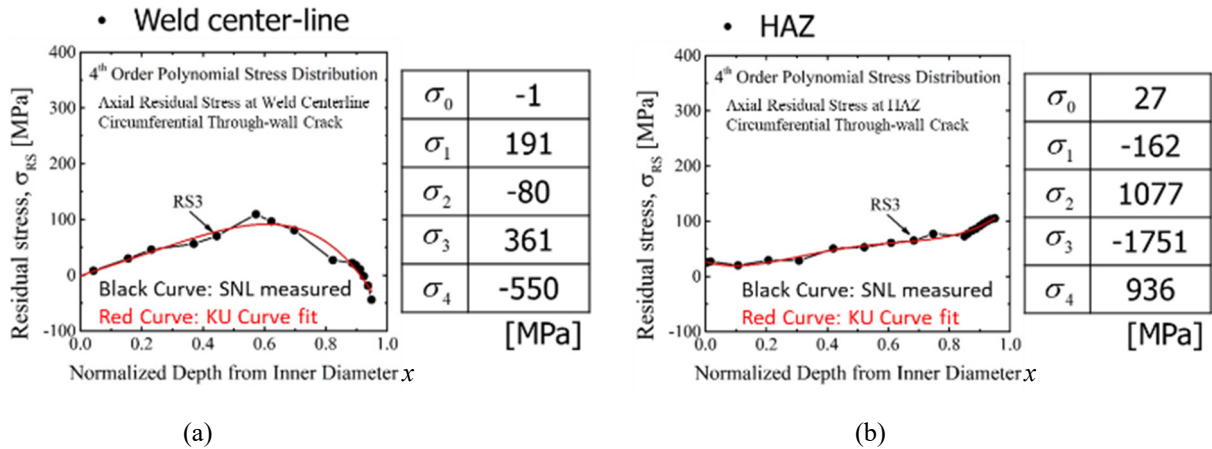


**FIGURE 9:** CURVE-FITTING OF THE WELDING RESIDUAL STRESSES AT WCL (a) AND IN HAZ (b): WRS PERPENDICULAR TO THE CIRCUMFERENTIAL WELD: RS3;  $x=0$  AT THE CANISTER INNER SURFACE  
(Courtesy of Korea University under I-NERI/USA-ROK [1, 13])

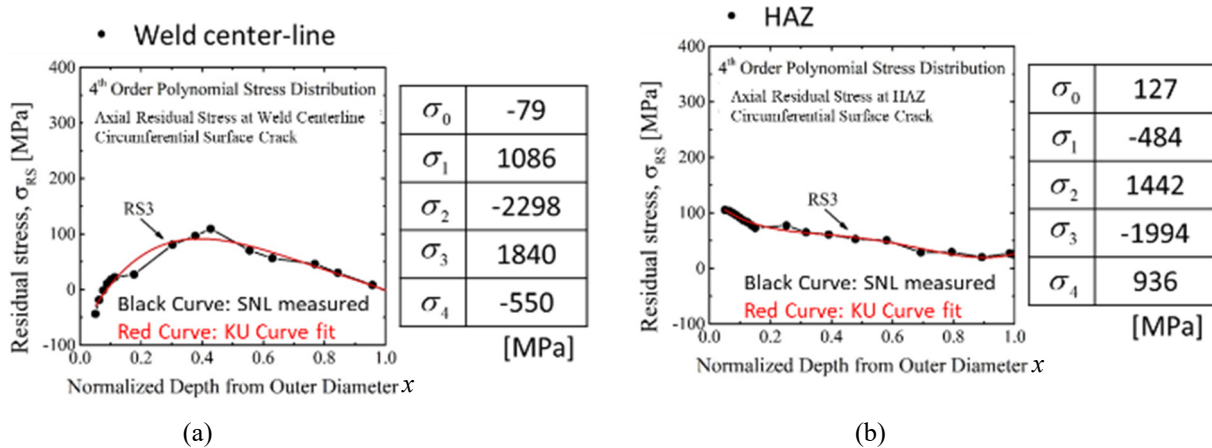


**FIGURE 10:** CURVE-FITTING OF THE WELDING RESIDUAL STRESSES AT WCL (A) AND IN HAZ (B): WRS PERPENDICULAR TO THE CIRCUMFERENTIAL WELD: RS3;  $x=0$  AT THE CANISTER OUTER SURFACE  
(Courtesy of Korea University under I-NERI/USA-ROK [1, 13])

The calculation results from (i) to (iv) above are summarized in Figure 11, where  $K$  is the value of  $K_I$  at each of the crack tip of the starter crack.

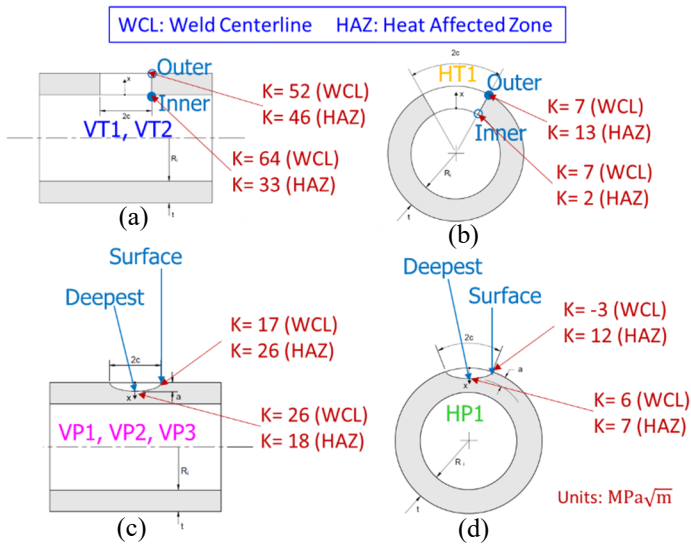


**FIGURE 11:** STRESS INTENSITY FACTORS OF THE STARTER CRACKS IN THE RESIDUAL STRESS FIELDS FOR A CIRCUMFERENTIAL WELD IN THE MOCKUP CANISTER: (a) VT1, VT2: THROUGH-WALL CRACK ACROSS THE WELD; (b) HT1: THROUGH-WALL CRACK PARALLEL TO THE WELD EDGE; (c) VP1, VP2, VP3: SEMI-CIRCULAR PART-THROUGH-WALL CRACK PERPENDICULAR TO THE WELD EDGE; (d) HP1: SEMI-CIRCULAR PART-THROUGH-WALL CRACK PARALLEL TO THE WELD EDGE

A collection of natural exposure field test data obtained by Kosaki [14] on Miyakojima Island, Japan indicated that the SCC could take place at a load as low as  $K_I = 1.0 \text{ MPa}\sqrt{\text{m}}$ . In addition, the laboratory immersion test in 5% salinity artificial seawater at  $50^\circ\text{C}$  conducted recently by Jeong et al. at KU [3,15,16] showed that the threshold value for the stress intensity factor was about  $15 \text{ MPa}\sqrt{\text{m}}$ . This implies that the  $K_{ISCC}$  of the canister materials exposed to marine environments could be between 1.0 and  $15 \text{ MPa}\sqrt{\text{m}}$ . Therefore, based on the calculation results in Figure 11, CISC could occur in the large plate, especially for the starter cracks perpendicular to the weld (Figures 11a and 11c), if the as-fabricated WRS was not significantly altered or relieved by the plate-sectioning from the mockup canister and by machining for starter cracks. However, the incubation time for the stress corrosion cracks to initiate in this material-environmental system is unknown.

Two EDM starter cracks (VP2 and HP1) have later been isolated in late October 2019 for a simultaneous experiment with extra salt loading (Figure 12). Additional liquid formed from the extra salts that have deliquesced. Significant corrosion activity has been observed - the presence of a brown-colored liquid (Figure 12b), presumably an iron-rich solution, has formed at one end of one of the two starter cracks with the increased salt

load. All starter cracks are being monitored visually. No visible indications of cracking have been observed after five months since the extra salt load was applied to the two selected starter cracks.

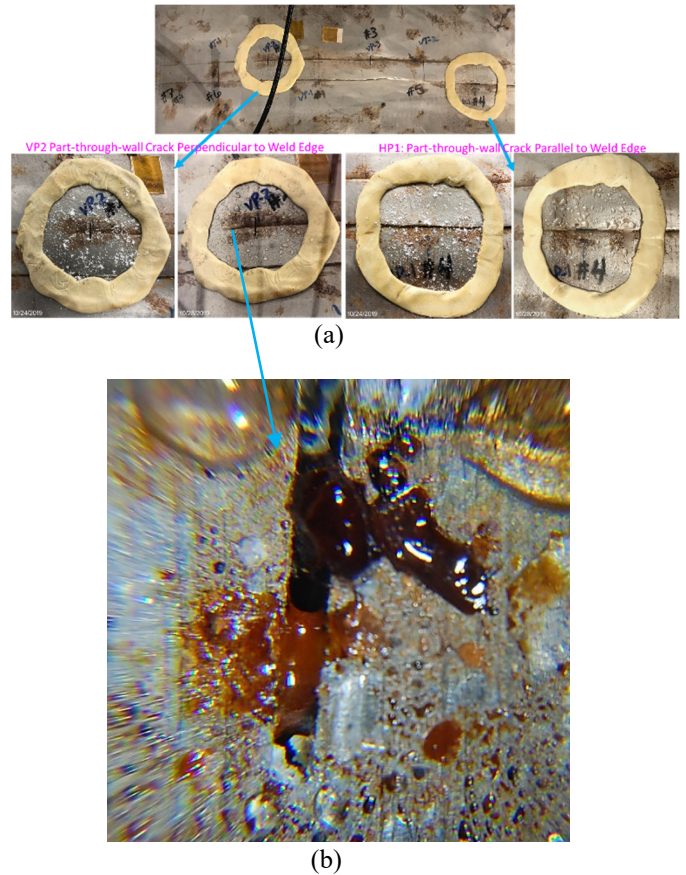


**FIGURE 12:** ADDITIONAL SALT LOADING OF EDM STARTER CRACKS VP2 AND HP1 (a) AND THE CLOSEUP OF CRACK VP2 (b)

## 5. CONCLUDING REMARKS

A large plate (approximately  $51 \times 46 \text{ cm}$ ) has been sectioned from a full-size mockup canister [1] in a region containing a circumferential weld. Starter cracks were fabricated by EDM in the weld region of the plate. It is used to demonstrate stress corrosion cracking under naturally deliquescing condition of dry salt in 75% relative humidity at room temperature. Periodic examination of the plate was planned by employing NDE techniques. Based on stress intensity factor calculations, the starter cracks were expected to grow, provided that the as-fabricated welding residual stress was not significantly altered or redistributed by plate sectioning from the mockup canister and by EDM of the starter cracks. The large plate test has been in progress since May 2019. General corrosion is continuously active in the vicinity of each crack, but no evidence of stress corrosion cracking has been observed on the plate surface.

## ACKNOWLEDGEMENTS

This work was sponsored by the Spent Fuel and Waste Science and Technology (SFWS) R&D Campaign, Office of Nuclear Energy under the U.S. Department of Energy, and by the Savannah River Nuclear Solutions, LLC under Contract No. DE-AC09-08SR22470 with the U.S. Department of Energy.

## REFERENCES

- [1] Enos, D. G. and Bryan, C. R., 2016, *Final report: Characterization of Canister Mockup Weld Residual Stresses*, FCRD-UFD-2016-000064 Sandia National Laboratories, Albuquerque, New Mexico, USA.
- [2] API 579-1/ASME FFS-1, 2007, *Fitness-For-Service (API 579 Second Edition)*, American Petroleum Institute, Washington, DC., USA.
- [3] Lam, P. S., Duncan, A. J., Ward, L. N., Sindelar, R. L., Kim, Y. J., Jeong, J. Y., Lee, H. J., and Lee, M. W., 2019, "Crack Growth Rate Testing and Large Plate Demonstration under Chloride-Induced Stress Corrosion Cracking Conditions in Stainless Steel Canisters for Storage of Spent Nuclear Fuel," Paper Number PVP2019-94031, Proceedings of the ASME Pressure Vessels & Piping Conference, San Antonio, Texas, USA.
- [4] Sindelar, R. L., Carter, J. T., Duncan, A. J., Garcia-Diaz, B. L., Lam, P. S., and Wiersma, B. J., 2016, "Chloride-Induced Stress Corrosion Crack Growth under Dry Salt Conditions – Application to Evaluate Growth Rates in Multipurpose Canisters," Paper No. PVP2016-63884, Proceedings of the ASME Pressure Vessels & Piping Conference, Vancouver, BC, Canada.
- [5] Duncan, A. J., Lam, P. S., Sindelar, R. L., and Carter, J. T., 2017, "Crack Growth Rate Testing with Instrumented Bolt-Load Compact Tension Specimens under Chloride-Induced Stress Corrosion Cracking Conditions in Spent Nuclear Fuel Canisters," Paper No. PVP2017-66105, Proceedings of the ASME Pressure Vessels & Piping Conference, Waikoloa, Hawaii, USA.
- [6] Duncan, A. J., Lam, P. S., Sindelar, R. L., and Metzger, K. E., 2018, "Crack Growth Rate Testing of Bolt-Load Compact Tension Specimens under Chloride-Induced Stress Corrosion Cracking Conditions in Spent Nuclear Fuel Canisters," Paper Number PVP2018-84753, Proceedings of the ASME Pressure Vessels & Piping Conference, Prague, Czech Republic.
- [7] Lam, P. S., Chang, C., Chao, Y. J., Sindelar, R. L., Stefek, T. M., and Elder III, J. B., 2005, "Stress Corrosion Cracking of Carbon Steel Weldments," Paper Number PVP2005-71327, Proceedings of ASME Pressure Vessels and Piping Conference, Denver, Colorado, USA.
- [8] Lam, P. S., 2009, *Investigation of the Potential for Caustic Stress Corrosion Cracking of A537 Carbon Steel Nuclear Waste Tanks*, SRNS-STI-2009-00564 Rev.1, Savannah River Nuclear Solutions, Aiken, South Carolina, USA.
- [9] Lam, P. S., Stripling, C. S., Fisher, D. L., and Elder III, J. B., 2010, "Potential for Stress Corrosion Cracking of A537 Carbon Steel Nuclear Waste Tanks Containing Highly Caustic Solutions," Paper No. PVP2010-25117, Proceedings of ASME Pressure Vessels and Piping Conference, Bellevue, Washington, USA.
- [10] Wang, J. A., Payzant, A., Bunn, J., and An, K., 2018, *Neutron Residual Stress mapping for Spent Nuclear Fuel Storage Canister Weldment*, ORNL/TM-2018/827, Oak Ridge, Tennessee, USA.
- [11] Gim, J. M., Kim, J. S., Kim, Y. J., and Lam, P. S., 2018, "FE welding residual stress analysis and validation for spent nuclear fuel canisters," Paper Number PVP2018-84857, Proceedings ASME Pressure Vessels & Piping Conference, Prague, Czech Republic.
- [12] Shirai, K., Tani, J., Arai, T., Wataru, M., Takeda, H., and Saegusa, T., 2011, "SCC Evaluation of Multi SCC Evaluation of Multi-Purpose Canister," Proceedings of 2011 International Radioactive Waste Management Conference (IHLRWMC), Albuquerque, New Mexico, April 10–14, Paper No. 3333.
- [13] Lam, P. S. and Kim, Y. J., 2016, *Flaw Stability and Stress Corrosion Cracking of Austenitic Stainless Steel Canisters for Long Term Storage and Transportation of LWR Used Fuel*, I-NERI Project Number 2016-001-K, U. S. Department of Energy, Office of Nuclear Energy, Washington D. C., USA.
- [14] Kosaki, A., 2006, "SCC Propagation Rate of Type 304, 304L Steels under Oceanic Air Environment," Paper No. ICONE14-89271, Vol. 1, Plant Operations, Maintenance and Life Cycle; Component Reliability and Materials Issues; Codes, Standards, Licensing and Regulatory Issues; Fuel Cycle and High Level Waste Management, International Conference on Nuclear Engineering, July 17-20, Miami, Florida, USA, pp. 443-450
- [15] Jeong, J. Y., Lee, M. W., Kim, Y. J., Sindelar, R. L., and Duncan, A. J., "Development of an Apparatus for Chloride Induced Stress Corrosion Cracking Test Using Immersion Method with Constant Displacement Condition," Paper Number PVP2019-93922, Proceedings of the ASME Pressure Vessels & Piping Conference, San Antonio, Texas, USA, July 2019.
- [16] Jeong, J. Y., Lee, M. W., Kim, Y. J., Lam, P. S., and Duncan, A. J., "Development of a Tester for Accurate Measurement of Chloride Induced Stress Corrosion Crack Growth Rate," submitted for publication to ASTM Journal of Testing and Evaluation, February 2020.